EXPERIMENTAL DATABASE WITH REAL PROPELLANTS TO STUDY MULTI-PHASE FLUID HAMMER PHENOMENA

J. Anthoine*, J-Y. Lestrade

ONERA - The French Aerospace Lab
F-31410, Mauzac, France
* jerome.anthoine@onera.fr

J. Steelant

ESA-ESTEC
2200 AG Noordwijk, The Netherlands

ABSTRACT

The objective of the present study is to generate a reliable experimental database on the fluid hammer phenomenon with real propellants (MMH and NTO) to validate the physical models implemented in the numerical codes. This database with real propellants extends the database obtained by the von Karman Institute on similitude fluids (water, ethanol and acetaldehyde). The test facility is composed with parts provided by VKI (propellant line, fast opening valve, measurement module and instrumentation). The combination of these elements with the Onera pressure vessel and vacuum system enables to build a facility close to the VKI one used for similitude fluids. For each real propellant, experiments were performed for a vacuum pressure in the propellant line below and above the saturation pressure of the fluid to highlight the influence of the physical phenomena encountered (vaporisation, cavitation …) on the fluid hammer. With MMH, the higher is the vacuum pressure, the smaller are the fluid hammer frequency and amplitude. The same conclusions found by VKI for ethanol when compared to water are now found with MMH: the fluid hammer amplitude is smaller and the frequency is higher. Only one experiment was performed with NTO for a vacuum pipe pressure below the saturation pressure due to leaks of the valve seals. Compared to MMH and water experiments performed under the same operating conditions, the fluid hammer amplitude and frequency are smaller. Regarding the temperature, very small variations are recorded for water and MMH while the temperature increase for NTO is higher than 350°C.

NOMENCLATURE

ESPSS	European Space Propulsion System Simulation
FOV	Fast Opening Valve
MMH	MonoMethyl Hydrazine
NCG	Non Condensable Gas
N_2H_4	Hydrazine
NTO	Nitrogen TetrOxide
VKI	von Karman Institute

INTRODUCTION

The operation of spacecraft propulsion systems generally consists of four phases. The first one includes the launch and the separation of the satellite from the launcher vehicle. During this phase, the spacecraft propulsion system is inactive and the propellant tanks are isolated from the combustion chamber by at least two barriers: the latch valve which is a pyrotechnic valve and the propellant flow valve installed before the combustion chamber (figure 1). The second phase consists of the pressurization of the tanks and of the opening of the latch valve. From this stage, the propellant lines of the spacecraft, initially vacuum pumped or filled with a non-condensable gas at low pressure, are filled and pressurized. These operations are called “priming” and once achieved, the propulsion system is fully operational. The third phase or “drift orbit” takes place during the full deployment of the satellite where the propulsion system is used for attitude control and for positioning to the target orbit. Finally, the last phase or the “on station phase” consists of keeping the spacecraft in its orbit until the end of its operation lifetime.

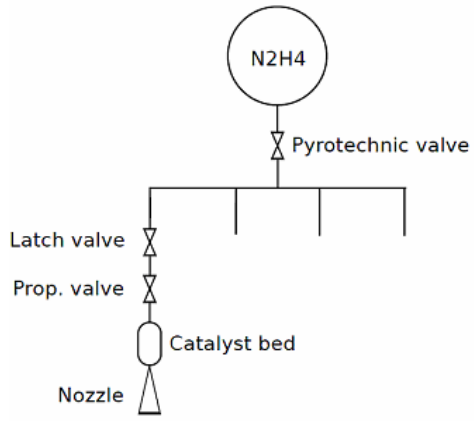

Figure 1: Spacecraft monopropellant propulsion system

The main problems encountered during the spacecraft lifetime are linked to the priming operation of the propulsion systems which is regularly faced with adverse fluid hammering effects classically known as water hammer. This operation may turn out to be

critical if the corresponding overpressures are not correctly considered in the pipe and sub-system dimensioning (flow control valve, pressure sensors, filters …).

The Propulsion Laboratory of Onera has already investigated experimentally the fluid hammer effects using simplified liquid (water) and real propellants into several pipe configurations, where the liquid was pressurized in a tank and the pipe system was vacuum pumped [1]. A pressure surge of 28.9 MPa is reached using water as the working fluid, starting from initial conditions of 2 MPa in the tank and 1000 Pa in the vacuum-pumped propellant line. Tests and results using MMH and NTO are presented and discussed. However, several phenomena, such as cavitation, absorption and desorption of a pressurizing gas and influence of the vapour generation, are not addressed during the study.

In a second study, still at Onera, the influence of the pressure ratio between the pipe and the tank, cavitation phenomenon and NCG content was investigated using ethanol, MMH, and acetaldehyde [2]. An adiabatic compression takes place at the end of the pipe when the liquid front is travelling downstream. The first peak presents a multiple step evolution explained by the generation of a two-phase flow at the front location. These studies proved that complementary fundamental experimental investigations are necessary for a better understanding of the phenomena which were not accounted for as the cavitation … Indeed, these multi-phase phenomena make the fluid-hammer behaviour hard to model due to a lack of the understanding of the physical processes taking place.

Within his PhD Thesis supported by ESA at VKI, Lema [3] performed a numerical investigation of the water hammer using the one-dimensional commercial software EcosimPro/ESPSS. Mixing layers develop between the pure liquid and pure air front, with vapour formation due to the cavitation phenomenon [4]. The driving pressure gas dissolved in the liquid leads to significant differences on the first pressure peak due to the speed of sound change. The commercial code CFD-ACE+ was also used with the full cavitation model and the simulations confirm high sensitivity of the water hammer prediction regarding the amount of NCG present in the liquid [5].

Within the ESA contract to support the PhD Thesis of Lema, VKI built a dedicated facility, representing a structural configuration of a propulsion system for typical satellite applications, with accurate control of the operating conditions [3,6-7]. The facility allows for the fundamental experimental investigation of the multi-phase fluid hammer and related multi-phase phenomena such as cavitation, boiling front, absorption and desorption of non condensable gases. It is constituted by a pressure vessel, a valve with an opening time lower than 30 ms and a given length of the propellant line. The facility includes a vacuum system to set the initial test conditions. Straight, elbow and T junction configurations are considered using real hardware provided by TAS-Cannes and Astrium Ottobrun. Similitude fluids such as water, ethanol and acetaldehyde are successively tested, the last two being respectively the similitude fluids for MMH and NTO. The characterisation of the wave front induced by the fluid hammer is achieved through a measurement module placed at the end of the test section. The module is instrumented with flush mounted dynamic transducers for unsteady measurements of pressure and temperature. The measurement module can also be replaced by a transparent one for flow visualisations with high speed imaging.

The VKI experimental database is built up by varying the vacuum conditions in the line, the saturation conditions of the test liquid, the pipe configuration and the liquid properties. Lema [3] found that the residual gas is responsible for attenuating the pressure raise due to its cushioning effect. The comparison of the results for the three liquids (water, ethanol and acetaldehyde) in the straight configuration shows that, besides the desorption rate, density and speed of sound appear as the key liquid properties, without a clear influence of the vapour pressure on the water hammer phenomenon. Lema [3] characterized also, for the first time, the water hammer phenomenon through flow visualizations. The quality of the recorded images is impressive and the sequence of snapshots allows distinguishing the foamy mixture preceding the liquid front and the non condensable gas compression when the front impacts at the bottom end. The same sequence shows also the subsequent column separation with the creation of bubbles and the impact of that separated liquid column against the bottom end.

The understanding of this multi-phase behaviour and the creation of the VKI extensive experimental database in case of simulating fluids allowed the validation and the improvement of the physical models implemented in EcosimPro/ESPSS and CFD-ACE, two numerical codes used by ESA to simulate fluid hammer phenomenon. To guaranty the reliability on these two numerical tools, it was proposed to complete the VKI experimental database with real propellants (MMH and NTO). Nevertheless, VKI does not have the certification to work with these two fluids. The chosen option was to perform the complementary experiments with real propellants at the Propulsion Laboratory of Onera which has the necessary certification and which has proven its mastery of these fluids in the past.

The paper firstly focuses on the description of the experimental facility which uses parts fulfilled by VKI. Then, the results of the fluid hammer experiments performed with real propellants are provided.

TEST FACILITY DESCRIPTION

The experiments performed by Onera made use of exactly the same hardware than VKI (propellant line, valves, measurement modules) [6], except the pressure vessel and the facility configuration: horizontal instead of vertical (for security reasons linked to real propellants). The test facility is then composed of a pressure vessel, a bent pipe, the VKI FOV and the VKI 2 m long propellant line (figure 2). The pressure vessel can be isolated from the bent pipe thanks to a valve allowing for the vessel filling (by replacing the bent pipe with a filling pipe). The bent pipe, linking the vessel to the FOV, includes a "T" to connect the service operation line allowing the vacuum pumping of the main line before the experiment and the blowing of the feeding line after. The vacuum of the pipe is achieved thanks to a vacuum pump which is placed after two cold traps allowing to reach a vacuum level around 500 Pa and to prevent vapour extraction by condensing these gaseous products. A pressurisation control panel enables to pressurise the tank and to regulate its pressure during the experiments.

The propellant pipe ends with a P-T measurement module provided by VKI (figure 3). The unsteady pressure probes (PCB) and the thermocouple were also provided by VKI. A first pressure probe (PCB1) is located at the beginning of the propellant line, just after the FOV and another one (PCB3) is added to measure the radial pressure close to the rear-end of the module located in the rear-end of the module. A last pressure probe (PCB2) measuring the fluid hammer amplitude and a thermocouple are located on the rear-end of the module.

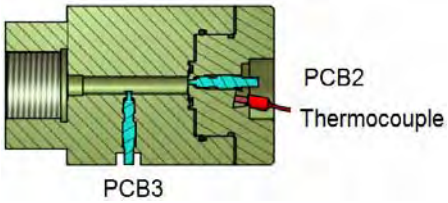

Figure 3: P-T measurement module

TEST MATRIX

In spacecraft, the liquid propellants are stored in a safety vessel pressurised at high pressure (2 MPa) before launch. All the pipes in the network are vacuum pumped at very low pressure (below 1000 Pa) or filled with NCG. The pipe pressure may then be either above or below the saturation pressure of the liquid propellants involving consequently different physical phenomena. So, for water and each propellant (MMH and NTO), experiments are performed with an initial pipe pressure below and above the saturation pressure of the liquid (Table 1). Considering the saturation pressure of water and MMH, the tests are achieved with vacuum pressure of 1000 and 10000 Pa in the pipe. Because of its high saturation pressure, the experiments with NTO are only performed with a vacuum pressure of 1000 Pa. To estimate the reproducibility of the phenomena, three successful tests for each experimental configuration are planned with a constant vessel pressure of 2 MPa.

Table 1: Saturation pressure of fluids at 293 K

H_2O	MMH	NTO
2340 Pa	4940 Pa	95830 Pa

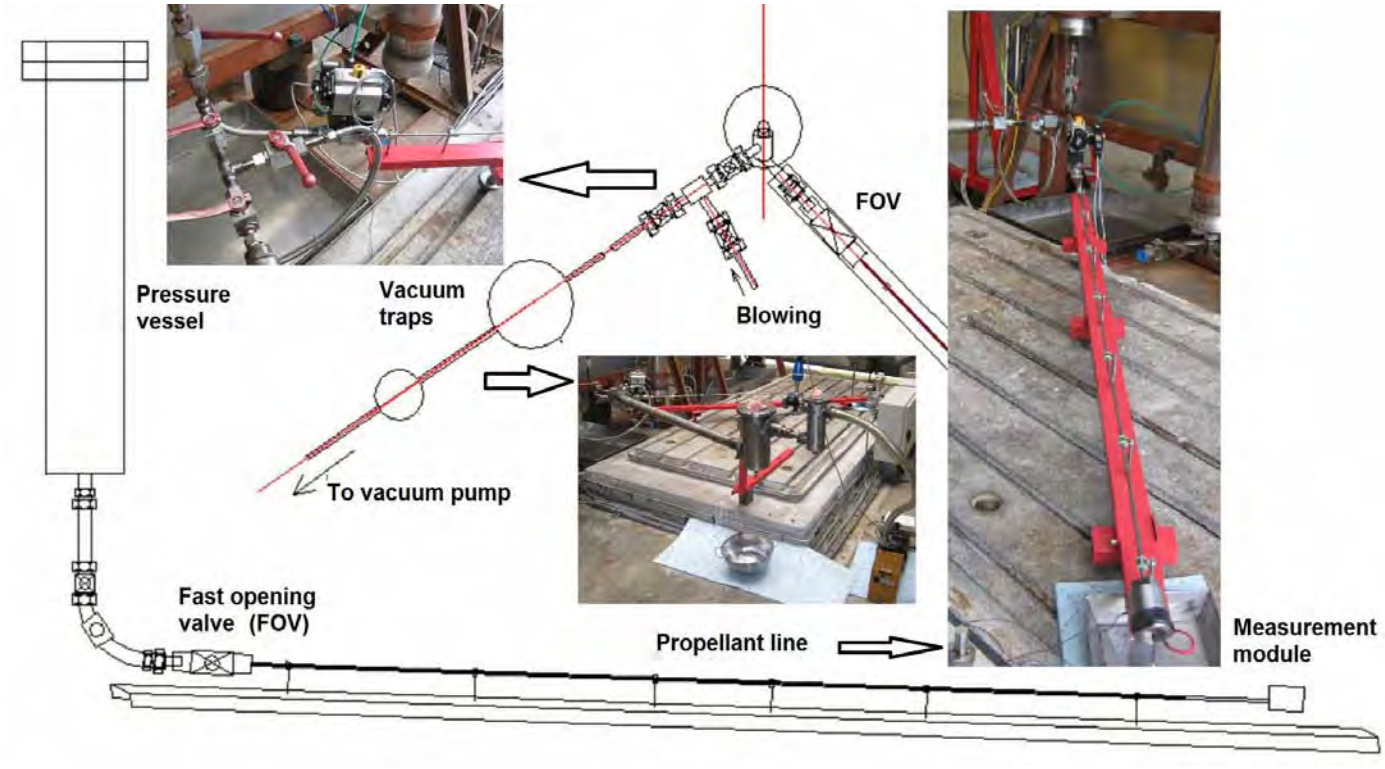

Figure 2: Test facility at Onera for the study of the fluid hammer phenomenon

EXPERIMENTAL RESULTS

Experiments Performed with Water

Figure 4 provides the experimental results obtained with water for a vacuum pressure of 1000 Pa in the pipe and for a tank pressure close to 2 MPa. The water hammer reaches a pressure of 28 MPa which rapidly decreases to the tank pressure value. Secondary oscillations appear during the main peak (figure 4b), which may be due to a mechanical oscillation of the back part of the module that contains the thermocouple since this part is screwed to unplug the module for the seal and thermocouple replacements. The radial pressure at the beginning of the module is nearly 60 % lower than the water hammer pressure measured at the rear-end of the module but the pressure evolutions are the same. The difference is certainly due to the existence of a vapour phase and the fact that the line is nearly horizontal (figure 2). As shown in figure 4a, the water hammer phenomenon can also be observed on the temperature measurement but its variation is very low.

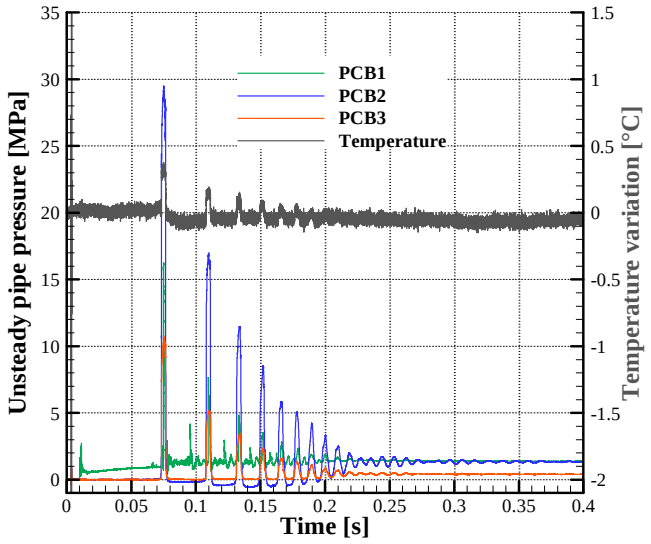

(a) Unsteady pipe pressure and temperature evolution

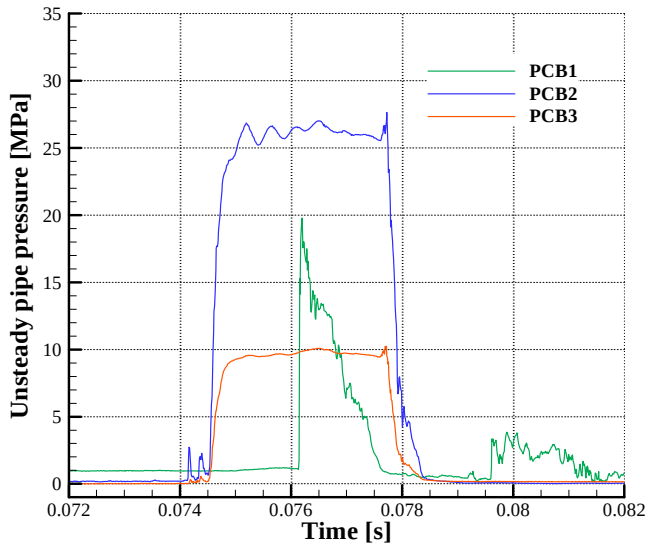

(b) Zoom on the first water hammer peak

Figure 4: Experiment performed with water for a vacuum pressure of 1000 Pa

Figure 5 shows a very good overlap of the first water hammer for the three tests, proving a good reproducibility of the phenomenon. The time axis of the results is corrected in order to assign the opening time of the FOV to 10 ms. This correction enables to underline the propagation time of the fluid from the FOV to the rear-end of the module which is specified in table 2 for the three tests. The knowledge of this propagation time enables to estimate the mean velocity of the fluid in the pipe which, for the three tests, is between 30 and 35 m/s.

Table 2: Propagation time of the fluid in the pipe for experiments performed with water

Experiment	Vacuum pressure of 1000 Pa	Vacuum pressure of 10000 Pa
a	63 ms	65 ms
b	63 ms	65 ms
c	63 ms	64 ms

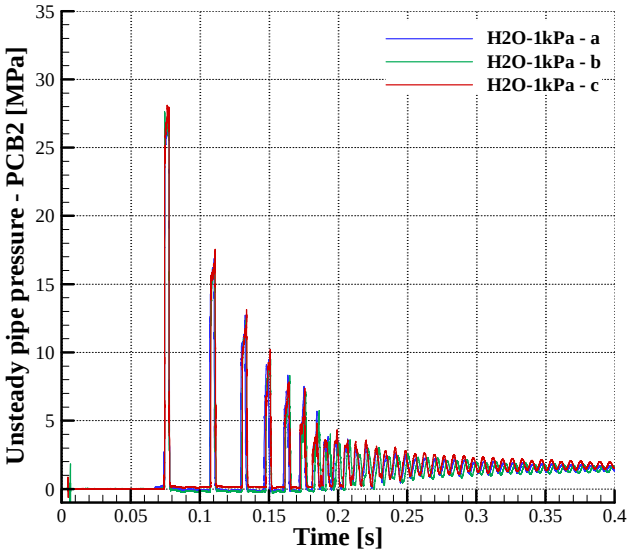

(a) Unsteady pipe pressure evolution

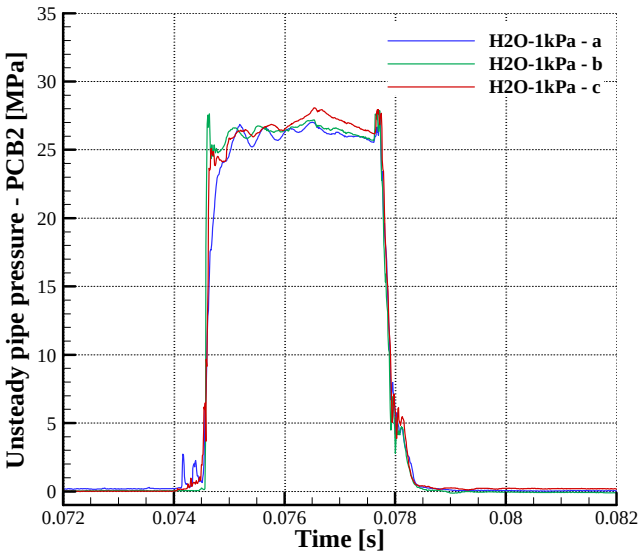

(b) Zoom on the first water hammer peak

Figure 5: Reproducibility of experiments performed with water for a vacuum pressure of 1000 Pa

Experiments Performed with MMH

Figure 6 provides the experimental results obtained with MMH for a vacuum pressure of 1000 Pa in the pipe and for a tank pressure close to 2 MPa. The fluid hammer reaches a pressure of 27 MPa. As for water experiments, the first fluid hammer peak presents secondary oscillations (figure 6b) which seem higher than previously. The fluid hammer is also visible on the temperature measurement but its variation is again very small (figure 6a). The behaviour is however different since the temperature decreases at the beginning of the fluid hammer. The reproducibility of the three tests is still very good which leads to a good overlap of the first fluid hammer (figure 6b) and to similar propagation times of MMH in the feeding line (table 3).

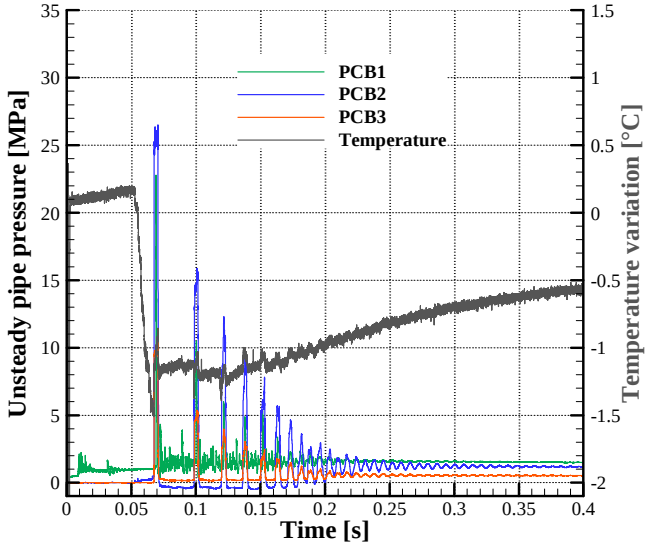

(a) Unsteady pipe pressure and temperature evolution

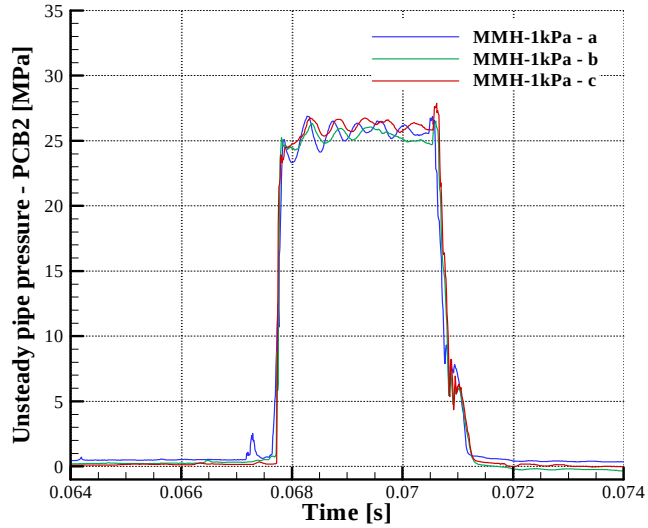

(b) Zoom on the first fluid hammer peak

Figure 6: Reproducibility of experiments performed with MMH for a vacuum pressure of 1000 Pa

The second series of MMH experiments, for a vacuum pressure of 10000 Pa in the pipe and a tank pressure of 2 MPa, is shown in figure 7. In these conditions, the fluid hammer reaches about 26 MPa and, as for the previous experiments, the temperature decreases when the first fluid hammer occurs and its variation is not significant. The reproducibility of the three tests is still very good which leads to a good overlap of the first fluid hammer (figure 7b) and to similar propagation times of MMH in the feeding line (table 3).

Table 3: Propagation time of the fluid in the pipe for experiments performed with MMH

Experiment	Vacuum pressure of 1000 Pa	Vacuum pressure of 10000 Pa
a	57 ms	59 ms
b	57 ms	59 ms
c	56 ms	60 ms

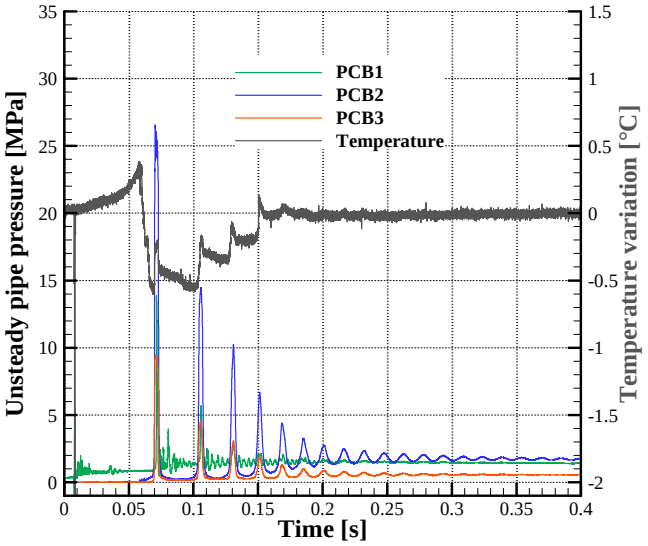

(a) Unsteady pipe pressure and temperature evolution

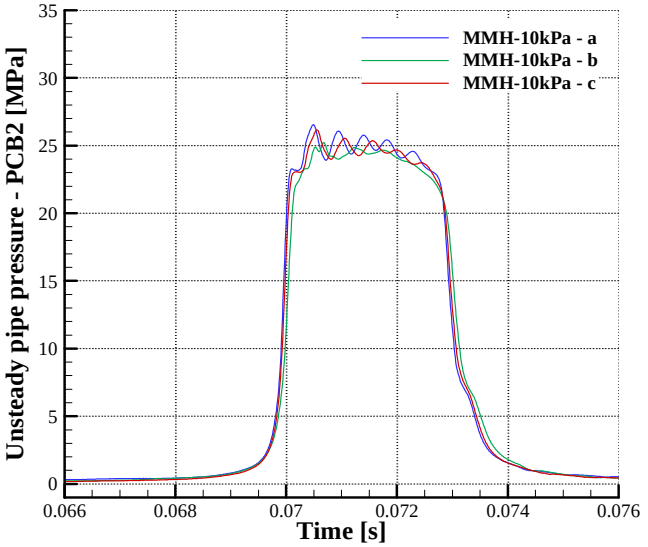

(b) Zoom on the first fluid hammer peak

Figure 7: Reproducibility of experiments performed with MMH for a vacuum pressure of 1000 Pa

Experiments Performed with NTO

Due to the corrosive aspect of NTO, experiments with this propellant were difficult to perform. Even though the valves for service operation, vacuum pumping and blowing were refurbished with seals compatible with NTO, the propellant dissolved them causing leaks.

Consequently, just one experiment was realised with a vacuum pipe pressure below the saturation pressure of NTO (1000 Pa) and for a tank pressure close to 2 MPa. Under these conditions, the fluid hammer at the rear-end of the measurement module reaches about 19 MPa and, as for the tests performed with water and MMH, the radial pressure measured at the beginning of the module (PCB3) is about 60% lower than the previous one (figure 7). The fluid hammer is, once again, visible on the temperature measurement but, contrary to the previous experiments, the variation of the temperature is higher than 350°C and can not be completely estimated since the data were overloaded.

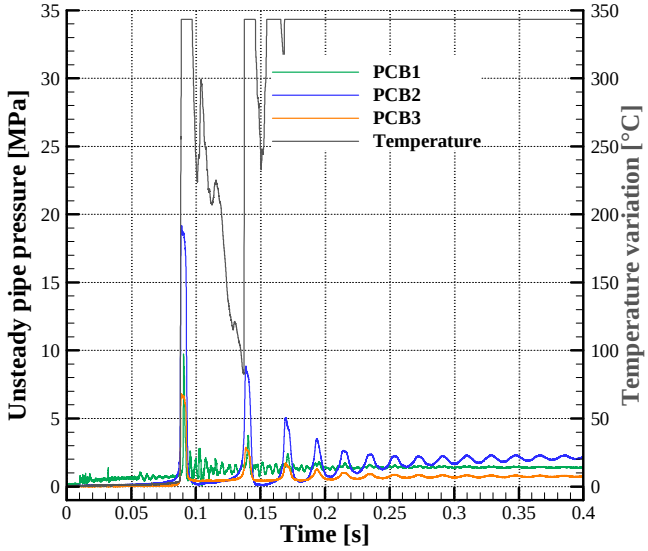

Figure 8: Experiment performed with NTO for a vacuum pressure of 1000 Pa

Test Comparison

When comparing the experiments performed with MMH, the higher is the vacuum pressure of the pipe, the smaller are the frequency and the amplitude of the fluid hammer phenomenon (figure 9). Moreover, the fluid hammers appear before with a vacuum pipe pressure of 1 kPa than with 10 kPa. These conclusions are consistent with the conclusions drawn by VKI from the experiments with ethanol.

By comparison to experiments performed with water, experiments achieved with MMH have a lower fluid hammer amplitude but a higher peak frequency (figure 9). This conclusion is consistent with the one of the comparison of VKI experiments performed with water and ethanol. On the contrary, the experiment with NTO has a much lower fluid hammer amplitude and a lower peak frequency compared to water and MMH (figure 9).

Finally, figure 10 collects the maximum pressure of the fluid hammer for all the experiments performed at Onera. Even though the absolute value of the first pressure peak is much smaller for NTO than for water and MMH, the amplitudes of the different peaks appear on the same curve for both real fluids (MMH and NTO) in the (max-amplitude, time) diagram. The results for water appear on a parallel curve associated to higher pressure in the same diagram and this is valid for both vacuum pipe pressures.

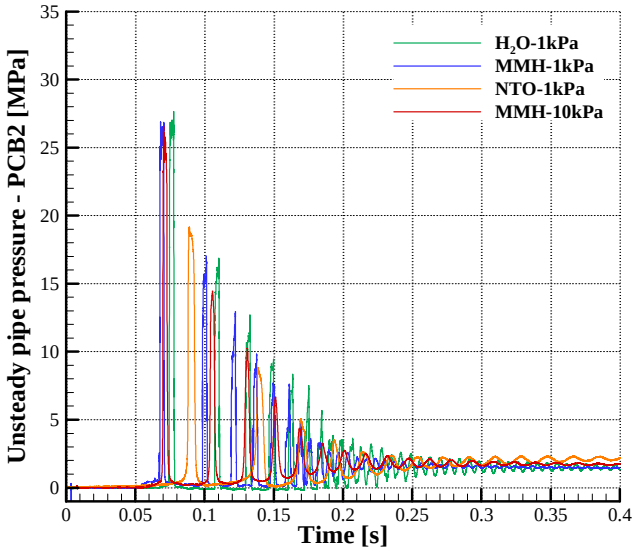

(a) Unsteady pipe pressure evolution

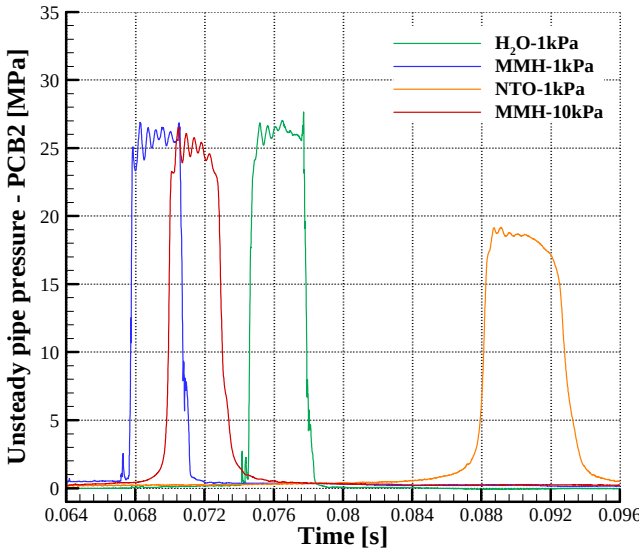

(b) Zoom on the first fluid hammer peak

Figure 9: Comparison of experimental data between water, MMH and NTO

CONCLUSIONS

The experimental database on multi-phase fluid hammer phenomena, obtained by the von Karman Institute for inert fluids, has been extended by Onera for real propellants (MMH and NTO). The same facility hardware downstream of the FOV was used, i.e. FOV, propellant line and measurement modules, but the propellant line was installed horizontally instead of vertically (at VKI).

For a vessel pressure of 2 MPa and a vacuum pressure in the pipe of 1000 Pa, the amplitudes of the fluid hammer are equal to 27 MPa for MMH and to 20 MPa for NTO. For MMH, the higher is the vacuum pressure of the feeding line, the smaller are the frequency and the amplitude of the fluid hammer phenomenon.

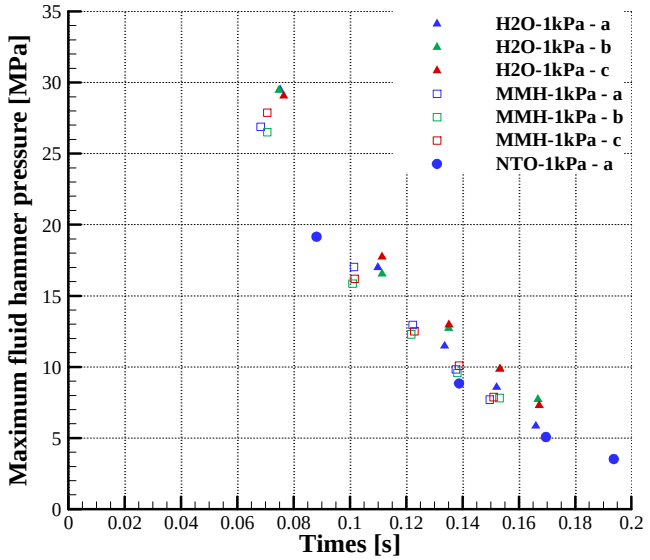

(a) Vacuum pressure in the pipe of 1000 Pa

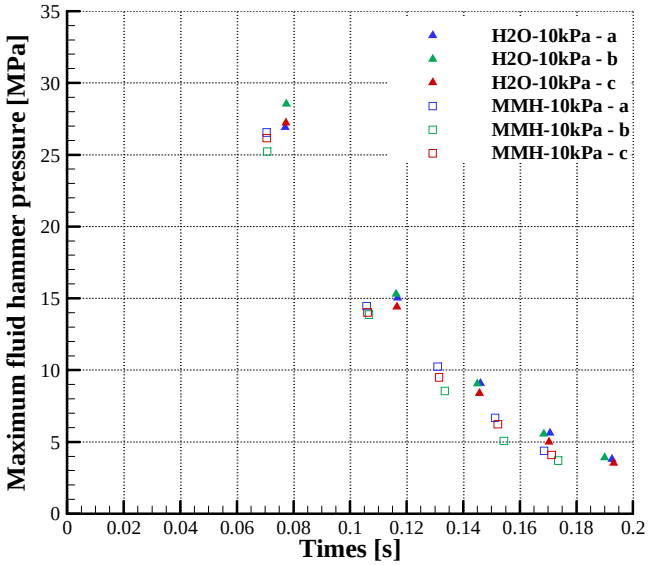

(b) Vacuum pressure in the pipe of 1000 Pa

Figure 10: Comparison of maximum fluid hammer pressure between water, MMH and NTO

The same conclusions for MMH compared to water can be drawn than for ethanol: the fluid hammer amplitude is lower and the frequency is higher for MMH. The experiment with NTO has a much lower fluid hammer amplitude and a lower peak frequency compared to water and MMH. The amplitudes of the different fluid hammer peaks appear however on the same curve for both real fluids (MMH and NTO) in the (max-amplitude, time) diagram.

Regarding the temperature, very small variations are recorded for water and MMH while the temperature increase for NTO is higher than 350°C. Further temperature measurements with NTO are necessary to confirm this value, as well as with acetaldehyde as similitude fluid.

Some visualizations were also performed in order to have a better understanding of the physics involved in the multi-phase fluid hammer phenomenon. However, when adjusting the visualisation settings, the VKI visualization module has been broken prohibiting the achievement of promising visualizations with real propellants. Further work would require manufacturing a new module and performing further visualisations.

ACKNOWLEDGMENT

This study is supported by the ESA through the General Support Technology Programme activity AO/1-6210/09/NL/CP. The authors would like to thank J-M. Buchlin, P. Rambaud and M. Lema from VKI for their collaboration within this project.

REFERENCES

[1] Gibek, I. and Maisonneuve, Y., "Water Hammer Tests with Real Propellants," *41th AIAA/ASME/ SAE/ASEE Joint Propulsion Conference and Exhibit*, July 2005, AIAA Paper 2005-4081.

[2] Lecourt, R. and Steelant, J., "Experimental Investigation of Waterhammer in Simplified Feed Lines of Satellite Propulsion Systems," *Journal of Propulsion and Power*, Vol. 23, No. 6, 2007, pp. 1214-1224.

[3] Lema, M., "Multiphase Fluid Hammer: Modeling, Experiments and Simulations," PhD Thesis, Université Libre de Bruxelles, 2013.

[4] Porca, P., Lema, M., Rambaud, P. and Steelant, J., "Experimental and Numerical Multiphase-Front Fluid Hammer," *Journal of Propulsion and Power*, Vol. 30, No. 2, 2014, pp. 368-376.

[5] Pinho, J., Lema, M., Rambaud, P. and Steelant, J., "Multiphase Investigation of Water Hammer Phenomenon Using the Full Cavitation Model," *Journal of Propulsion and Power*, Vol. 30, No. 1, 2014, pp. 105-113.

[6] Lema, M., Steelant, J., Peña, F. L. and Rambaud, P., "Multiphase Fluid Hammer in Spacecraft Propulsion Systems," *47th AIAA/ASME/ SAE/ASEE Joint Propulsion Conference and Exhibit*, July 2011, AIAA Paper 2011-5683.

[7] Lema, M., Steelant, J., Lopez, F.P. and Rambaud, P., "Experimental Characterization of the Priming Phase Using a Propellant Line Mock-up," *Space Propulsion 2012*, Bordeaux, France, May 2012.